Check for updates

Received: 29 June 2022 | Accepted: 19 September 2022

DOI: 10.1002/pip.3630

RESEARCH ARTICLE

PROGRESS IN PHOTOVOLTAICS WILEY

Interlaboratory comparison of voltage sweep methods used for the electrical characterization of encapsulated high-efficiency c-Si solar cells

Yating Zhang[1] | Christos Monokroussos[1] | Harrison Wilterdink[2] | Harald Müllejans[3] | Diego Pavanello[3] | Masahiro Yoshita[4] | Kengo Yamagoe[4] | Klaus Ramspeck[5] | David Hinken[6] | Karsten Bothe[6] | Yuji Fujita[7] | Gilles Arnoux[8] | Filipe Pinto[8] | Rajesh Ambigapathy[8] | Qi Gao[9] | Qiang Shi[9] | Yi Feng Chen[10] | Yan Ping[10]

[1]TÜV Rheinland (Shanghai) Co., Ltd., Shanghai, China

[2]Sinton Instruments, Boulder, Colorado, USA

[3]European Commission*, Joint Research Centre (JRC), Ispra, Italy

[4]Renewable Energy Research Center (RENRC), National Institute of Advanced Industrial Science and Technology (AIST), Tsukuba, Ibaraki, Japan

[5]h.a.l.m. elektronik GmbH, Frankfurt am Main, Germany

[6]Institute for Solar Energy Research GmbH (ISFH), Emmerthal, Germany

[7]Kyoshin Electric Co., Ltd., Kyoto, Japan

[8]PASAN SA (Meyer Burger Group), Neuchatel, Switzerland

[9]Shanghai Institute of Microsystem and Information Technology, Chinese Academy of Sciences, Shanghai, China

[10]Trina Solar Co., Ltd., Changzhou, Jiangsu, China

Correspondence
Christos Monokroussos, TÜV Rheinland (Shanghai) Co., Ltd., Shanghai, China.
Email: christos.monokroussos@tuv.com

Abstract

This work presents the comparison of measurement results for four types of encapsulated high-efficiency c-Si solar cells measured by 10 laboratories based in Asia, Europe and North America utilizing a wide range of voltage sweeping methods, which include well-established procedures that represent good industry practice, as well as recently introduced ones that have not been verified yet. The aim of the round-robin interlaboratory comparison was to examine the measurement comparability of different laboratories with respect to their measurement methods of high-efficiency solar cells. A proficiency test was employed to examine the consistency of results and their corresponding uncertainties. The short-circuit current (I_{SC}) under STC measured by four accredited laboratories was firstly compared. In order to investigate the consistency related to the high device capacitance, the value of the I_{SC} was fixed for all 10 participants. The results of all participant laboratories—compared via E_n number analysis—generally remained well within [−1; 1], thus indicating consistency between the measured values and the reference values within stated measurement uncertainties. The differences remained within ±1.15% in P_{MAX} and within ±0.35% in V_{OC} for all participants and methods applied. Correlations were observed among the P_{MAX}, V_{OC}, and *FF* differences from their weighted mean. An analysis of the effects of transient current (dQ/dt) at maximum power point caused by hysteresis effect on the measurement error of P_{MAX} showed a significant linear correlation between error of maximum power and junction voltage sweep rate for heterojunction (HJT) solar cells. This work forms the basis to validate all applied methods and their stated measurement uncertainties.

KEYWORDS
characterization, electrical performance, high-efficiency c-Si solar cell, hysteresis effect, interlaboratory comparison, round-robin, transient current

The views expressed are purely those of Harald Müllejans and Diego Pavanello and may not in any circumstances be regarded as stating an official position of the European Commission.

 © 2022 John Wiley & Sons Ltd.

1099159x, 0, Downloaded from https://onlinelibrary.wiley.com/doi/10.1002/pip.3630 by Universite Lorraine, Wiley Online Library on [04/11/2022]. See the Terms and Conditions (https://onlinelibrary.wiley.com/terms-and-conditions) on Wiley Online Library for rules of use; OA articles are governed by the applicable Creative Commons License

1 | INTRODUCTION

The power measurements of high-efficiency (HE) c-Si technologies have been a challenge for both production lines and calibration laboratories for decades.[1–3] HE c-Si devices exhibit measurement deviations due to their slow response causing hysteresis in *I*–*V* measurements in particular when using pulsed solar simulators. However, pulsed solar simulators are much more common as they are significantly cheaper and easier to use when compared to steady-state solar simulators. With pulsed solar simulators, the time for measuring an *I*–*V* curve within a single sweep is typically limited to about 10 ms, resulting in deviations between the measured electrical performances of HE PV devices with respect to their performance under steady-state illumination. Such deviations are attributed to the diffusion capacitance of c-Si devices, which derives from the redistribution of charge carriers in the depletion region of the pn-junction under forward bias. HE c-Si have longer diffusion lengths for minority carriers and hence would also have a higher innate diffusion capacitance than conventional solar cells, giving rise to measurement deviations. Such deviations have been reported previously for both solar simulators and outdoor measurements.[1–6]

Recent developments in HE c-Si technologies (such as *p*-type passivated emitter rear contact [PERC], *n*-type passivated emitter rear totally diffused [PERT], heterojunction [HJT], and interdigitated back contact [IBC]) have popularized these devices in the market and made the accuracy of their calibration increasingly important. In parallel, advances in measurement systems have opened new possibilities for characterization[7–12] in addition to proven standard procedures involving long-pulse solar simulators, the multi-flash method, and steady-state conditions such as those provided by natural sunlight or steady-state solar simulators.

A preliminary analysis of this round-robin interlaboratory comparison has been presented in Monokroussos et al[13] and was extended in this work based on more data and further analysis. The aim of this work is to examine the comparability of measurements of different laboratories utilizing different procedures for the measurement of HE solar cells with a particular focus on voltage sweeping methods. The sweeping methods utilized by the participants of the round-robin are (i) linear sweep rate; (ii) nonlinear sweep rate; (iii) hysteresis measuring and correction; (iv) voltage-stepping correction; and (v) voltage-irradiance modulation and correction. This work is also intended to compare different methods and laboratory setups used between ISO/IEC 17025 accredited calibration and testing laboratories as well as industrial laboratories that have processes and procedures in place in accordance with IEC 60904-1.[14] The correlations and their statistical significance between P_{MAX}, V_{OC}, and *FF* differences from their weighted mean are then calculated. Additionally, the relation between transient current at maximum power point caused by hysteresis effect and error of maximum power value is investigated. In this context, an HE-encapsulated solar cell round-robin was initiated and is presented together with the data analysis in the following sections.

2 | METHODOLOGY

2.1 | Participant laboratories, measurement uncertainty, and setups

A round-robin was realized between 10 laboratories based in Asia, Europe, and North America. The participants were five ISO/IEC 17025 accredited laboratories (three for calibration and two for testing) and five industrial laboratories. Namely, the participant laboratories were AIST (Japan), Berger Lichttechnik (Germany), JRC ESTI (Italy), h.a.l.m. elektronik (Germany), ISFH (Germany), Kyoshin Electric Co., Ltd. (Japan), Pasan, Meyer Burger (Switzerland), SIMIT, CAS (China), Sinton Instruments (USA), and TÜV Rheinland (China). The participant laboratories employed one or more of the abovementioned sweeping methods to electrically characterize the devices under test (DUTs). Table 1 lists information related to the accreditation but also the method and the sweeping procedure that each of the participant laboratories employed. Five laboratories applied the linear step-like method, which was implemented by adjusting the voltage sweeping ramp on steady-state or long-pulse solar simulator. When the illumination length of solar simulator is limited, several different methods were utilized:

1. Nonlinear voltage stepping method[8,10]; the innovation of this method is to allocate more time for *I*–*V* data points with larger capacitive effects.
2. Voltage-irradiance modulation[7]; the terminal voltage of the solar cell is modulated in real time to maintain a constant charge in the solar cell cells, and thus, the capacitive effect during the *I*–*V* sweeping is compensated.
3. Correction methods[11,12]; the implementation of this method is usually based on multiple *I*–*V* curves, such as a set of illuminated and their corresponding dark *I*–*V* curves or the forward and backward *I*–*V* curves. The relationship between multiple *I*–*V* curves is analyzed, and equations will be deduced to correct the measured *I*–*V* curves.

Measurement uncertainty in HE PV devices is driven by devices' hysteresis and reference irradiance. As both effects can impact the I_{SC}, P_{MAX}, and V_{OC} of the DUTs, it is desirable to design an experiment that can isolate the influence of reference irradiance calibration, so measurement deviations can be directly associated with device hysteresis and consequently the voltage sweeping strategy employed. In order to do so, predetermined I_{SC} values were assigned to each of the DUTs by the initiator and communicated to all participants in advance. All laboratories were then asked to perform *I*–*V* characterization of the DUTs so that the I_{SC} matches the predefined value while controlling device temperature at (25 ± 1)°C. In addition to the measurement under predetermined I_{SC} values, four ISO/IEC 17025 accredited laboratories also provided the measurement results of HE solar cells under STC for comparability. All participants employed four-terminal connections, while the contact points for voltage and current were clearly marked, so one may assume that deviations due to contacting played a secondary role.

1099159x, 0, Downloaded from https://onlinelibrary.wiley.com/doi/10.1002/pip.3630 by Universite Lorraine, Wiley Online Library on [04/11/2022]. See the Terms and Conditions (https://onlinelibrary.wiley.com/terms-and-conditions) on Wiley Online Library for rules of use; OA articles are governed by the applicable Creative Commons License

TABLE 1 List of participant laboratories, methods, and *I*–*V* sweeping procedures employed in the round-robin

Lab. participants	Accreditation	Illumination (min. pulse length)	IV sweeping method	Sweeping direction
AIST (Japan)	ISO/IEC 17025 for calibration	Long-pulse solar simulator (>100 ms)	Linear sweep	From I_{SC} to V_{OC}
Berger Lichttechnik (Germany)	None	Pulse solar simulator (>10 ms)	Linear step-like	From I_{SC} to V_{OC}
CAS, SIMIT (China)	ISO/IEC 17025 for testing	Long-pulse solar simulator (>100 ms)	Linear step-like	From I_{SC} to V_{OC}
JRC ESTI (Italy)	ISO/IEC 17025 for calibration	Steady-state solar simulator (>1 s)	Linear step-like	From I_{SC} to V_{OC}
h.a.l.m. elektronik (Germany)	None	Pulse solar simulator (>110 ms)	Advanced Hysteresis[12] 1. 2 × 16 ms (hysteresis) 2. 2 × 24 ms (hysteresis) 3. 2 × 50 ms (hysteresis) 4. 2 × 110 ms (hyst./multiflash) 5. 2 × 2,500 ms (hyst./multiflash)	From I_{SC} to V_{OC} and From V_{OC} to I_{SC}
ISFH (Germany)	ISO/IEC 17025 for calibration	Steady-state solar simulator (>10 s)	Linear sweep	From I_{SC} to V_{OC}
Kyoshin Electric Co., Ltd. (Japan)	None	Pulse solar simulator (>20 ms)	1. Multiflash 2. Photo and dark analysis (hysteresis)[11] 3. Fast and versatile (nonlinear sweep)	1. From I_{SC} to V_{OC} 2. From I_{SC} to V_{OC} and from V_{OC} to I_{SC} 3. From I_{SC} to V_{OC} and from V_{OC} to I_{SC}
Meyer Burger, Pasan (Switzerland)	None	Pulse solar simulator (>10 ms)	1. *Dragonback*® (nonlinear voltage stepping)[10] 2. Smart Sweep (nonlinear sweep)	1. From I_{SC} to V_{OC} 2. From I_{SC} to V_{OC}
Sinton Instruments (USA)	None	Pulse solar simulator (multiple flashes of >1 ms)	Voltage-irradiance modulation[7]	N/A
TÜV Rheinland (China)	ISO/IEC 17025 for testing	1. Pulse solar simulator A (>10 ms) 2. Pulse solar simulator B (>80 ms)	Dynamic I–V (nonlinear voltage stepping)[8]	1. From I_{SC} to V_{OC} 2. From I_{SC} to V_{OC}

The aim of measurement of PV devices is to determine their electrical performance under steady-state illumination. In this context, a comparison of I_{SC} values under STC indicates the deviations between different accredited laboratories in terms of the traceability of the reference irradiance, spectral mismatch, nonuniformity of irradiance, and measurement setups for HE solar cells. A comparison of P_{MAX} and V_{OC} under predetermined I_{SC} reveals deviations arising from device hysteresis, due to the different voltage sweeping strategies employed without influence from irradiance traceability and spectral mismatch correction. This strategy effectively allows to isolate and quantify measurement deviations due to device hysteresis. The measurement uncertainty contributions (UCs) for the electrical parameters at predefined I_{SC} values and STC and are reported in Tables 2 and 3, respectively.

2.2 | DUTs

The DUTs were four types of encapsulated HE c-Si solar cells (two types of *p*-type PERC and two types of *n*-type HJT) with initial aperture solar cell efficiencies varying between 20.5% and 23.1%. In total, 11 single-cell encapsulated devices were used in the round-robin, seven of which were measured by all participants, while four were kept by the initiator in a controlled environment of temperature, humidity, and light and were used as control cells (one per type). More details about the test specimens are given in Table 4. Prior to any measurements, all samples were subject to (15–25) kWh/m^2 light soaking in accordance with the stabilization procedures listed in IEC 61215-2. Therefore, all devices were sufficiently stabilized prior to the round-robin.

2.3 | Interlaboratory comparison approach and project time flow

The interlaboratory comparison took place from June 2018 to July 2020. The round-robin approach was employed here, that is, the test samples were measured in turn by each participant and shipped to the subsequent laboratory. The agreed test protocol required electrical characterization and the I_{SC} of the DUT matches its predefined value

1099159x, 0, Downloaded from https://onlinelibrary.wiley.com/doi/10.1002/pip.3630 by Universite Lorraine, Wiley Online Library on [04/11/2022]. See the Terms and Conditions (https://onlinelibrary.wiley.com/terms-and-conditions) on Wiley Online Library for rules of use; OA articles are governed by the applicable Creative Commons License

TABLE 2 Laboratory measurement uncertainty contributions (UCs) of electrical parameters at predefined I_{SC} values ($k = 2$)

	P_{MAX}	V_{oc}
AIST	0.30%	0.30%
Berger Lichttechnik	0.70%	0.50%
JRC ESTI	0.75%	0.20%
h.a.l.m., 2 × 16 ms	0.60%	0.40%
h.a.l.m., 2 × 24 ms	0.60%	0.40%
h.a.l.m., 2 × 50 ms	0.60%	0.40%
h.a.l.m., Multiflash, 2 × 110 ms	0.60%	0.40%
h.a.l.m., Multiflash, 2 × 2500 ms	0.70%	0.50%
ISFH	0.70%	0.35%
Kyoshin Electric, FAV*	0.59%	0.30%
Kyoshin Electric, Multiflash	0.52%	0.30%
Kyoshin Electric, PDA**	0.55%	0.30%
Pasan, *Dragonback*	0.70%	0.50%
Pasan, Smart Sweep	1.50%	0.50%
Sinton Instruments	1.20%	0.70%
SIMIT, CAS	1.20%	0.70%
TÜV Rheinland	1.11%	0.40%

Note: For laboratories, which practiced measurements with multiple methods, the name of the method is indicated next to the laboratory name.

TABLE 3 Laboratory measurement uncertainty contributions (UCs) of electrical parameters at STC ($k = 2$)

	I_{SC}	P_{MAX}	V_{oc}
AIST	1.40%	1.40%	0.30%
JRC ESTI	0.70%	1.00%	0.20%
SIMIT, CAS	1.60%	2.00%	0.70%
TÜV Rheinland	1.50%	1.60%	0.70%

at 25°C. The predefined I_{SC} value of each DUT was assigned randomly within ±3% of the I_{SC} value at STC measured by the initiator. It is noted that different randomized offsets were applied for the assignment of predefined I_{SC} values per DUT type that varied within two standard deviations of measurement uncertainty of the initiator. This practice ensures that the participants could not deduct any systematic differences between devices by comparing the dispersion of values at predefined I_{SC}. Furthermore, four laboratories characterized the performance of solar cells under STC for comparability. Optionally, EL measurements were also taken for all samples, as long as the laboratory was qualified to do so. A time flow of the round-robin is shown in Table 5. The identity of participants is not disclosed to ensure the confidentiality of the results. Participant laboratories are rather identified with capital letters A–J assigned by order of testing. Due to shipment issues, the initiator laboratory (A) repeated its final measurements before laboratory (J) concluded the round-robin.

2.4 | Methods for statistical analysis

Interlaboratory measurement deviations of PV device electrical parameters are derived (in the most simple case) against the arithmetic average of participant laboratories.[15–17] The disadvantage of this approach is that it does weight all participants equally without considering the measurement UC of individual laboratories.

In this work, the reference values were assigned based on the weighted (by measurement uncertainty) average of all values of accredited calibration and qualifying testing laboratories. Several assumptions were made by this approach, that is, (i) the stated uncertainties were correct and valid; (ii) the approach using the weighted mean was justified; and (iii) all measurements were completely independent. This approach has been previously used successfully in other interlaboratory comparisons[17–20] and represents the state of the art, as it provides a higher weight to those values measured with lower uncertainty.

The disadvantage of such an approach is that it depends on each laboratory's stated uncertainties but also on the stability of DUTs. A reliable uncertainty estimate requires firstly traceability (i.e., an unbroken chain of prior measurements to international standards; see IEC 60904-4[21]), secondly a rigorous analysis of all possible contributions in the measurement itself, and thirdly a stable device, which would allow the direct interlaboratory comparison of measurements practiced by different laboratories.

2.4.1 | Proficiency test to assess the reliability

A validity and consistency of all results was firstly tested in order to identify and, if necessary, eliminate outliers. For this purpose, the values submitted by all participants were compared with a reference value, which was chosen as the weighted (by inverse square measurement uncertainty) average of all participant calibration laboratories according to ISO/IEC 17025. A proficiency test was performed employing E_n numbers in accordance with ISO/IEC 17043[22] as

$$E_{ni} = \frac{x_i - \bar{x}}{\sqrt{U_{95i}^2 + \bar{U}_{95}^2}} \quad (1)$$

E_{ni} is the E_n number of the ith participant laboratory, x_i is the measurement value corresponding to a measurement uncertainty U_{95i} of the ith participant laboratory. $\bar{x}$ is the consensus value with a measurement uncertainty $\bar{U}_{95}$. An agreement between results within stated UCs is obtained when the E_n number is between −1 and 1; the results do not agree with the reference within stated UCs if the E_n number is outside this range. Some causes for an erroneous measurement have to be excluded firstly, and then the UCs are reestimated and revised. Only those results passing this proficiency test and produced by ISO/IEC 17025 accredited laboratories are considered for the calculation of the weighted mean.

1099159x, 0, Downloaded from https://onlinelibrary.wiley.com/doi/10.1002/pip.3630 by Universite Lorraine, Wiley Online Library on [04/11/2022]. See the Terms and Conditions (https://onlinelibrary.wiley.com/terms-and-conditions) on Wiley Online Library for rules of use; OA articles are governed by the applicable Creative Commons License

TABLE 4 List of the encapsulated cells used in the round-robin together with their constructional characteristics

Sample no.	Use	Cell technology	Initial aperture solar cell efficiency[a]	Soldering/dimensions
HJT-1 #1	Round-robin	*n*-type HJT	~21.6%	Double soldered per +/− terminal; 20 × 20 cm
HJT-1 #2	Round-robin			
HJT-1 #3	Control			
HJT-2 #1	Round-robin	*n*-type HJT	~23.1%	Double soldered per +/− terminal; 38 × 38 cm
HJT-2 #2	Round-robin			
HJT-2 #3	Control			
PERC-1 #1	Round-robin	*p*-type PERC	~21.6%	Double soldered per +/− terminal; 30 × 30 cm
PERC-1 #2	Control			Single soldered per +/− terminal; 30 × 30 cm
PERC-2 #1	Round-robin	*p*-type PERC	~20.5%	Double soldered per +/− terminal; 30 × 30 cm
PERC-2 #2	Round-robin			Double soldered per +/− terminal; 30 × 30 cm
PERC-2 #3	Control			Single soldered per +/− terminal; 30 × 30 cm

[a]Initial aperture solar cell efficiency is calculated based on the initial nominal power after stabilization assuming the total projected area of the solar cell under test (which were at all cases ~15.6 × 15.6 cm), but excluding its surrounding area. It is given here indicatively of the total conversion solar cell efficiency. It is noted that the actual solar cell total conversion efficiency would be lower. As the surrounding area far exceeded the actual cell dimensions, there is a non-negligible part of light redirected toward the cell from its surroundings due to multiple internal reflections inside the glass, which raises the aperture solar cell efficiency.

TABLE 5 Time flow of measurement in the round robin between participant laboratories (A–J) highlighted with different color codes; different measurements sets performed by the initiator laboratory are marked with a number

Year	2018							2019					
Month	6	7	8	9	10	11	12	1	2	3	4	5	6
Lab.	A1	→			B	→	C	→	D	→	E	→	F	→	G
Year	2019					2020							
Month	7	8	9	10	11	12	1	2	3	4	5	6	7
Lab.	→	H		→		I	→		A2		→		J

Note: Interlaboratory shipment time is indicated with arrows and highlighted in gray.

2.4.2 | Consensus value and its uncertainty

The weighted mean represents the best estimate of the true value of the measurand. In the present interlaboratory comparison, it is calculated on the basis of results validated by the proficiency test as described above and chosen therefore as the consensus value from expert participant for each electrical parameter (either V_{OC} or P_{MAX}). For simplicity, hereafter, we will refer to this consensus value just as weighted mean.

In addition, corrections were applied to consider multiple results submitted by a single laboratory. In particular, Laboratory A measured all modules twice. Therefore, a formula accounting for both reliability weights (i.e., measurement uncertainty) and frequency weights (i.e., number of independent measurements submitted per laboratory) was employed. Specifically, the weighted mean, $\bar{x}$, of measurements was derived as follows[23,24]:

$$\bar{x} = \frac{\sum_{i=1}^{n} w_i x_i}{\sum_{i=1}^{n} w_i} \tag{2}$$

with weight w_i defined as

$$w_i = \frac{1}{N_{lab} \cdot U_{95i}{}^2} \tag{3}$$

and x_i is a measurement with expanded measurement uncertainty ($k = 2$), U_{95i}. In Equation (3), N_{lab} is the number of independent measurement sets submitted by each laboratory. The notation n represents the total number of independent measurements submitted by all participants in the round-robin. The derived values are considered as the best estimate of the true value of the electrical parameters.

The uncertainty of the weighted mean can then be expressed as[25]

$$\bar{U}_{95} = \frac{1}{\sqrt{\sum_{i=1}^{m} \frac{1}{U_{95i}{}^2}}} \tag{4}$$

The notation m represents the number of participant testing or calibration laboratories, that is, five in our case.

The uncertainty of the weighted mean is a deterministic quantity that depends only on predetermined quantities, that is, the stated measurement uncertainties, and does not convey stochastic information about the dispersion of measurements or the order of laboratory agreement.

Interlaboratory deviations were expressed in terms of weighted standard deviation to the weighted mean. This is a more conservative approach as compared to the maximum absolute difference between laboratories results because it accounts for the dispersion of

1099159x, 0, Downloaded from https://onlinelibrary.wiley.com/doi/10.1002/pip.3630 by Universite Lorraine, Wiley Online Library on [04/11/2022]. See the Terms and Conditions (https://onlinelibrary.wiley.com/terms-and-conditions) on Wiley Online Library for rules of use; OA articles are governed by the applicable Creative Commons License

measurements, and therefore, it can provide a more comprehensive estimate of laboratory agreement. The weighted standard deviation was used rather than the standard deviation, which gives higher statistical weight to differences measured with lower uncertainty. As the sample size was relatively small (<30), the unbiased estimator correction was used for the population variance.[26]

$$\bar{s}_w = \sqrt{\frac{\sum_{i=1}^{n} w_i (x_i - \bar{x})^2}{\sum_{i=1}^{n} w_i - \frac{\sum_{i=1}^{n} w_i^2}{\sum_{i=1}^{n} w_i}}} \quad (5)$$

where w_i, x_i, and $\bar{x}$ have the same meaning as introduced above.

2.4.3 | Results correlation and its significance

I_{SC}, V_{OC}, and P_{MAX} are known to be related.[17] Since I_{SC} values are predefined in this work, only the relation between V_{OC} and P_{MAX} is considered. The degree of linear dependence, if any, between variables is statistically evaluated by the Pearson correlation, ρ,[27] of a population. A correction is required for a limited sample when the entire population is unknown. In a series of n measurements x_i and y_i with i indicating the ith measurements, the sample correlation coefficient, $r_{x,y}$, can be used to approximate the population correlation, $\rho_{x,y}$. It is expressed mathematically as

$$r_{x,y} = \frac{\sum_{i=1}^{n} (x_i - \bar{x}) \cdot (y_i - \bar{y})}{\sqrt{\sum_{i=1}^{n} (x_i - \bar{x})^2 \cdot \sum_{i=1}^{n} (y_i - \bar{y})^2}} \quad (6)$$

The quantities $\bar{x}$ and $\bar{y}$ are the reference values of the measured quantities. Correlation coefficients close to 1 indicate a direct linear relation between the quantities x and y (1:1), that is, y is directly proportional to x. Correlation coefficients approaching to 0 correspond to uncorrelated quantities (0:1), that is, y is totally independent from x.

There are some weak but observable correlations reported in previous work[17]; it is difficult to differentiate between statistical randomness and a weak actual relationship. Therefore, the significance of a correlation has to be assessed. This is achieved in this work by following the Bayesian statistics approach,[27] which is based on the posterior probabilistic assessment of a null hypothesis, H_0, that in our case assumes uncorrelated quantities (i.e., $r_{x,y} = 0$). If the probability value (P-value) of H_0 is less than or equal to a critical probability, α, H_0 is rejected in favor of the alternative hypothesis, H_A, meaning the quantities are correlated. If the P-value of H_0 is greater than α, then H_0 is assessed true and H_A is rejected and the quantities under examination are assumed to be uncorrelated. The hypotheses that we consider are:

- Null hypothesis (H_0): $\rho = 0$
- Alternate hypothesis (H_A): $\rho \neq 0$ (H_A: $\rho > 0$)

It is noted that the possibility of anti-correlation (i.e., $\rho < 0$) is ruled out, as it would imply unphysical negative dependence between V_{OC} and P_{MAX}. Although anti-correlation may occur in the relation of V_{OC} and P_{MAX}, that is, when temperature varies significantly, in this interlaboratory comparison, the temperature was controlled strictly at (25 ± 1)°C by all participants. Therefore, only one-tailed statistics are considered for the calculation of corresponding P-values between V_{OC} and P_{MAX}. For the relation between FF and V_{OC} and P_{MAX}, two-tailed statistics, and the possibility of positive and negative correlations (i.e., $\rho < 0$ and $\rho > 0$), are considered.

The P-value is here calculated for the t-statistic of the test, and a comparison with a critical probability of $\alpha = 0.05$ (i.e., H_A has 95% critical significance) is made, which also aligns with margins of error of the uncertainty. A rejection of H_0 is triggered when the P-value of the hypothesis H_0 does not achieve critical significance, that is, $P_r(t|H_0) \leq 0.05$. For a linear regression t-test, the t-statistic is approximated as[28]

$$t = \frac{r_{x,y} \cdot \sqrt{v - 2}}{\sqrt{1 - r_{x,y}^2}} \quad (7)$$

where $v - 2$ are the degrees of freedom (i.e., the number of results submitted by all participants bound in our case by the two coefficients of the linear regression).

3 | RESULTS AND DISCUSSIONS

An analysis of the results is discussed in the following subsections in terms of:

1. stability of test samples (Section 3.1);
2. robustness of results (Section 3.2);
3. comparison of results under STC (Section 3.3);
4. interlaboratory deviations for the electrical performance parameters measured under predefined I_{SC} (Sections 3.4 and 3.5);
5. correlation between electrical performance parameters (Section 3.6); and
6. effect of transient current on the error of maximum power value (Section 3.7).

3.1 | Degradation, drift, or metastability of test samples

As device metastability, degradation, or drift would directly affect the outcome of the round-robin, it is important to minimize its impact. When this is not possible, it is equally important to be able to quantify any performance changes to isolate deviations deriving from hysteresis from those of device stability or drift in general. A possible change

1099159x, 0, Downloaded from https://onlinelibrary.wiley.com/doi/10.1002/pip.3630 by Universite Lorraine, Wiley Online Library on [04/11/2022]. See the Terms and Conditions (https://onlinelibrary.wiley.com/terms-and-conditions) on Wiley Online Library for rules of use; OA articles are governed by the applicable Creative Commons License

in device performance due to shipment or stability was investigated by monitoring the trend of electrical parameter deviation along with the chronological order of testing. To determine relative drifts in the performance of the test samples, a set of measurements was performed on all devices by the initial laboratory at the beginning and end of the round-robin. Additionally, EL images of each device were taken by each laboratory as a supplementary method to monitor the potential mechanical damage to the devices due to the shipment.

In general, most of the devices did not show noticeable damage with the exception of DUT HJT-2 #2. It sustained damage in its electrical termination while in Laboratory I. The damage was significant, as one of the electrical terminals was completely cut off (Figure 1), which changed the measured P_{MAX} on average by approximately 2.0% (see Figure 2). For this reason, the results of DUT HJT-2 #2 measured after damage occurred will not be accounted in the following analysis.

A relative comparison of performance parameters for samples PERC-2 #1 and #2 as measured by each laboratory in respect to the weighted average of all measurements is shown in Figure 3A. Samples PERC-2 #1 and #2 exhibited moderate systematic degradation behavior, which is noticeable in V_{OC} and P_{MAX}. Specifically, for device PERC-2 #1, P_{MAX} degraded approximately 1.10% and V_{OC} approximately 0.84%, while PERC-2 #2 degraded approximately 0.75% in P_{MAX} and 0.67% in V_{OC}. The estimates provided were based on the differences seen between initial and final measurements carried out by the initiator laboratory at STC (not predefined I_{SC}). The effect was also noticeable when comparing the EL images of this cell taken at the beginning and the end of the round-robin (as shown in Figure 4), which generally indicates an increase of series resistance or a decrease in the minority carrier lifetime. The increase of series resistance was ruled out, because a reduction of V_{OC} was also observed, but also because a comparison of EL images of the cell at higher and lower injection still showed a darkening of the cells. Therefore, it is assumed that minority lifetime changes influenced the degradation of cells PERC-2 #1 and #2. Interestingly, the control samples (which were stored in a dark environment) have not shown similar behavior,

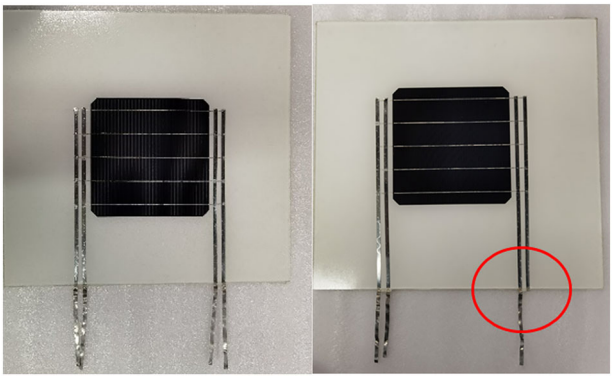

FIGURE 1 Sample HJT-2 #1 (left) and HJT-2 #2 (right) carrying double soldered electrical terminations. The sample HJT-2 experienced damage in its exterior terminations during the round-robin. [Colour figure can be viewed at wileyonlinelibrary.com]

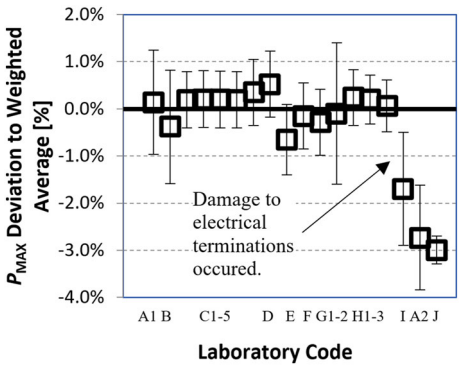

FIGURE 2 Maximum power deviation for DUT HJT-2 #2 as measured blindly by each laboratory at predefined I_{SC} condition at 25°C in respect to the weighted average of all measurements before any damage occurred. The measurements of the last three laboratories was not accounted in the weighted average calculation. X-axis denotes the test laboratory code in chronological order of testing. The estimated values of uncertainty ($k = 2$) are shown by error bars for each laboratory. The figure indicates the change after an electrical termination was accidentally cut off. [Colour figure can be viewed at wileyonlinelibrary.com]

pointing out that exposure to light (during electrical characterization measurements) may have an impact on the stability of the samples, even after the initial light soaking. Indeed, the control sample PERC-2 #3 was re-measured higher at STC by the initiator laboratory and its values changed by +0.23% in I_{SC} and +0.33% in P_{MAX}, which is within the laboratory reproducibility. In order to eliminate the degradation effect, a compensatory linear fit was applied, and the corrected V_{OC} deviation is shown in Figure 3B. The distribution of V_{OC} deviation after correction appears random between different laboratories, and the maximum deviation to the weighted average was within ±0.4%. It should be noted that the uncertainty due to this linear correction was not considered. In the following analysis on measurements under predefined I_{SC}, all the results related to DUT PERC-2 refer to the corrected values without the influence of degradation.

3.2 | Proficiency test: E_n numbers

The validity and consistency of electrical performance parameters were verified against reference values calculated through the weighted average of all participant accredited laboratories to identify and, if necessary, eliminate outliers. The results of this verification are expressed with E_n numbers for I_{SC}, P_{MAX}, and V_{OC} in Tables 6–8, respectively. It should be noted that the reported I_{SC} values were measured at STC by four accredited laboratories, while the P_{MAX} and V_{OC} values were measured under predetermined I_{SC} by all the participant laboratories. Since only two accredited laboratories provided I_{SC} results at STC of undamaged HJT-2 #2 cell, the results of DUT HJT-2 #2 cell were not included in Table 6.

As for results of I_{SC} measured at STC, the E_n numbers of laboratory J for DUTs HJT-2 #1 and PERC-2 #1 were out of [−1,1], and for

1099159x, 0, Downloaded from https://onlinelibrary.wiley.com/doi/10.1002/pip.3630 by Universite Lorraine, Wiley Online Library on [04/11/2022]. See the Terms and Conditions (https://onlinelibrary.wiley.com/terms-and-conditions) on Wiley Online Library for rules of use; OA articles are governed by the applicable Creative Commons License

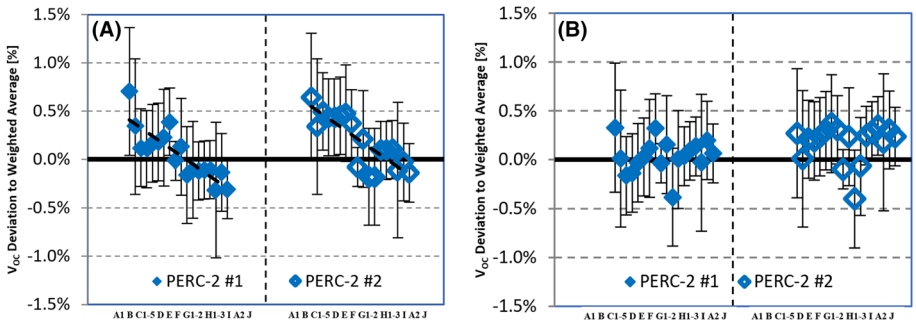

FIGURE 3 (A) Open-circuit voltage deviation for samples PERC-2 #1 and #2 as measured blindly by each laboratory at predefined I_{SC} condition at 25°C in respect to the weighted average of all measurements. X-axis denotes the test laboratory code in chronological order of testing. The estimated values of uncertainty ($k = 2$) are shown by error bars for each laboratory. The figure shows that samples PERC-2 #1 and #2 exhibited a linear degradation behavior during the course of round-robin. Dashed lines have been added as a guideline to show the linear regression of open-circuit voltages measured over time. (B) Open-circuit voltage deviation compared to the weighted average for samples PERC-2 #1 and #2 when the linear fit correction was used to compensate the effect of degradation. [Colour figure can be viewed at wileyonlinelibrary.com]

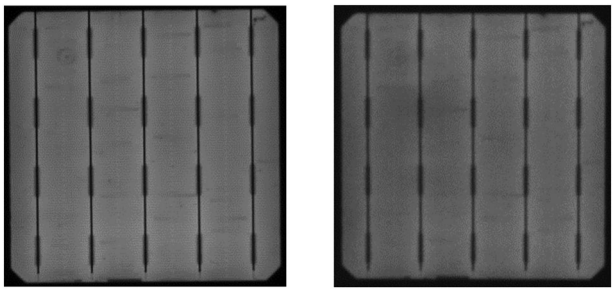

FIGURE 4 Sample PERC-2 #1 as measured by Laboratory B on 25 October 2018 and Laboratory A on 26 April 2020. A minor darkening of the image was observed, which indicates a decrease of minority carrier lifetime.

other DUTs, the lowest E_n numbers were corresponded to Laboratory J. The reason leads to this phenomenon will be discussed in Section 3.3. Two outliers were observed in the E_n numbers among all participants for P_{MAX}. Specifically, the measurements of Laboratory E for devices PERC-1 #1 and PERC-2 #2 were associated with an E_n number of −1.30 and −1.01, respectively. No outlier was observed for V_{OC}. The results of all participant laboratories generally remained well within [−1; 1], and the maximum absolute E_n numbers were 0.99 and 0.94 for P_{MAX} and V_{OC}, respectively. This result indicates consistency between the measured values and the reference values within the declared UCs for all measurement procedures and laboratories. All the results will be included in the subsequent comparison and analysis.

3.3 | Short-circuit current comparison under STC

In general, the accuracy of measured I_{SC} values mainly depends on the reference irradiance, which specifically refers to the calibration of the reference device, nonuniformity of irradiance on the test plane, and spectral mismatch calculation. In this inter-comparison round-robin, the reported uncertainties of secondary reference cells from four laboratories varied within 0.5%–1.0% ($k = 2$). The nonuniformity of irradiance on the test plane remained below 1% for all the participants. The spectral mismatch correction was applied in the reference irradiance calculation by all laboratories. A comparison of four laboratories in terms of the spectral response (SR) deviation of DUT HJT-1#1 with respect to the reference SR is taken as an example and shown in Figure 5. The reference SR represents here the arithmetic mean of all measurements. The majority of SR deviations from the reference value for HJT-1 #1 are within ±5% for each wavelength from 400 to 1100 nm, and these results are comparable for other module technologies. For a given spectral irradiance and reference device, the variability of spectral mismatch factor due to DUT SR measured by different laboratories is less than 0.3% for all the DUTs. From these values, it could be concluded that the influence of error of reference irradiance on the measured I_{SC} has been reduced largely for all four participant laboratories.

As shown in Figure 6, deviation of I_{SC} measured at STC against the weighted average was evaluated, and deviations remained within ±1.7% for all laboratories. The calculated uncertainty of the consensus value for I_{SC} remained 0.54% ($k = 2$) for all the modules, which mainly depends on the stated measurement uncertainties of all the participants rather than on module technology. The weighted deviation of DUTs, which represent the interlaboratory agreement, varied between 0.98% and 1.07% ($k = 2$) in I_{SC}. From these values, it could been seen that all the four accredited laboratories were in a relatively good agreement. However, there appears a noticeable decreasing trend in I_{SC} deviation along with time for all the module technologies. This phenomenon may be attributed to the stability issues on DUTs themselves over time or systematic errors of different laboratories, which happened to exhibit a diminishing trend under this sequence. Systematic errors, which arise either from the systematic electronic inaccuracies or the wrong implementation of test methods, will result in the consistent deviation from the true value. However, it is difficult

1099159x, 0, Downloaded from https://onlinelibrary.wiley.com/doi/10.1002/pip.3630 by Universite Lorraine, Wiley Online Library on [04/11/2022]. See the Terms and Conditions (https://onlinelibrary.wiley.com/terms-and-conditions) on Wiley Online Library for rules of use; OA articles are governed by the applicable Creative Commons License

TABLE 6 E_n numbers for I_{SC} for the participant laboratories at STC

Laboratory	HJT-1#1	HJT-1#2	HJT-2#1	PERC-1#1	PERC-2#1	PERC-2#2
E	0.28	0.28	0.69	0.51	0.66	0.82
I	0.02	−0.01	−0.31	−0.12	−0.42	−0.55
A2	−0.22	−0.15	−0.37	−0.46	−0.55	−0.69
J	−0.57	−0.58	−1.17	−0.88	−0.91	−1.10

TABLE 7 E_n numbers for P_{MAX} for the participant laboratories at predefined I_{SC} condition at 25°C

Laboratory	HJT-1#1	HJT-1#2	HJT-2#1	HJT-2#2	PERC-1#1	PERC-2#1	PERC-2#2
A1	0.53	0.22	0.59	0.11	0.28	0.27	0.06
B	0.08	0.09	−0.18	−0.30	0.32	0.13	0.09
C1	0.29	0.17	0.43	0.25	0.54	−0.20	0.10
C2	0.26	0.12	0.41	0.26	0.47	−0.16	0.10
C3	0.25	0.09	0.37	0.25	0.45	0.08	0.21
C4	0.21	0.07	0.35	0.25	0.49	0.08	0.32
C5	0.33	0.13	0.39	0.41	0.46	0.13	0.51
D	0.83	0.94	0.84	0.62	0.73	0.21	0.17
E	−0.58	−0.53	−0.77	−0.75	−1.30	−0.79	−1.01
F	0.39	0.38	−0.34	−0.19	0.99	0.42	0.48
G1	0.32	0.02	−0.19	−0.34	0.06	−0.23	−0.49
G2	0.09	0.24	−0.18	−0.13	0.51	0.30	−0.18
H1	0.59	0.97	0.67	0.31	0.64	0.01	0.38
H2	0.39	0.64	0.40	0.28	0.54	0.06	0.19
H3	0.18	0.51	0.42	0.08	0.54	0.19	0.43
I	0.60	0.48	0.99	-	0.14	0.10	0.23
A2	0.02	−0.12	−0.04	-	0.05	0.14	0.13
J	−0.10	−0.15	−0.04	-	0.16	0.00	0.03

TABLE 8 E_n numbers for V_{OC} for the participant laboratories at predefined I_{SC} condition at 25°C

Laboratory	HJT-1#1	HJT-1#2	HJT-2#1	HJT-2#2	PERC-1#1	PERC-2#1	PERC-2#2
A1	0.35	0.33	0.49	0.53	0.56	0.43	0.29
B	0.13	0.05	0.10	0.19	0.33	−0.04	−0.09
C1	0.34	0.04	0.55	0.61	0.71	−0.48	0.32
C2	0.34	0.08	0.55	0.77	0.50	−0.42	0.28
C3	0.40	0.14	0.58	0.86	0.36	−0.18	0.38
C4	0.40	0.11	0.55	0.83	0.64	−0.04	0.51
C5	0.38	0.25	0.55	0.76	0.49	0.14	0.56
D	0.62	0.74	0.71	0.84	0.94	0.73	0.59
E	−0.46	−0.47	−0.63	−0.54	−0.53	−0.36	−0.75
F	−0.11	−0.01	−0.05	0.08	0.46	0.20	0.29
G1	−0.21	−0.43	−0.65	−0.21	−0.25	−0.85	−0.94
G2	0.21	0.15	−0.31	−0.15	0.02	−0.10	−0.30
H1	0.43	0.66	0.66	0.58	0.47	−0.06	0.48
H2	0.41	0.44	0.33	0.59	0.47	0.10	0.62
H3	0.35	0.59	0.62	0.53	0.54	0.23	0.78
I	0.15	0.01	0.20	-	0.14	−0.28	0.26
A2	0.48	0.38	0.54	-	0.50	0.19	0.30
J	0.26	0.18	0.45	-	0.11	0.00	0.33

1099159x, 0, Downloaded from https://onlinelibrary.wiley.com/doi/10.1002/pip.3630 by Universite Lorraine, Wiley Online Library on [04/11/2022]. See the Terms and Conditions (https://onlinelibrary.wiley.com/terms-and-conditions) on Wiley Online Library for rules of use; OA articles are governed by the applicable Creative Commons License

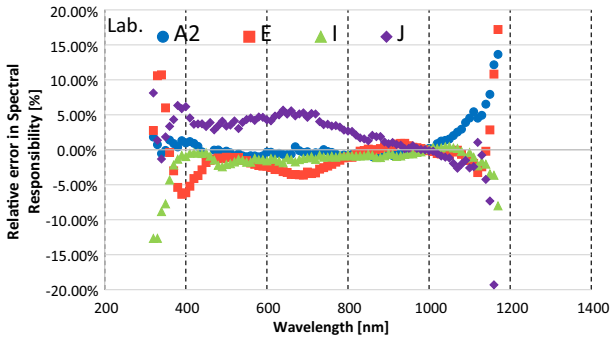

FIGURE 5 Deviations of SR with respect to the arithmetic mean of SRs for four participant laboratories. All data were interpolated and integrated in the range of 320–1180 nm, which is the SR range common to all participants. [Colour figure can be viewed at wileyonlinelibrary.com]

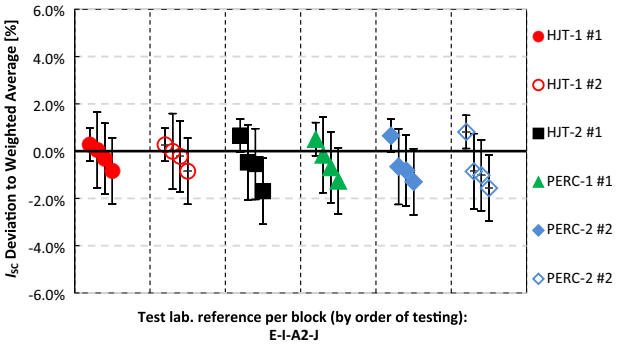

FIGURE 6 Short-circuit current deviations to the weighted mean as measured blindly by each laboratory at STC. The estimated values of measurement uncertainty ($k = 2$) are shown as error bars for each laboratory. [Colour figure can be viewed at wileyonlinelibrary.com]

to trace the origin of systematic errors when these errors are within the uncertainty of the measured values, which corresponds to the situation in this interlaboratory round-robin comparison.

3.4 | Maximum power comparison under predetermined I_{SC}

Interlaboratory deviations in P_{MAX} for each test sample as measured by all participant laboratories are shown in Figure 7. Since I_{SC} values were predefined, the weighted deviation for I_{SC} stayed below 0.06% ($k = 2$) for all modules, which shows that all calibrations have been carried out correctly for all modules. The worst-case agreement in I_{SC} has been −0.3%, which was measured by laboratory D for DUT PERC#2-1. This would introduce an error contribution to P_{MAX} by approximately −0.3% for Laboratory D.

The calculated uncertainty of the consensus value of P_{MAX} was 0.25% ($k = 2$) for all the modules. The weighted deviation of DUTs

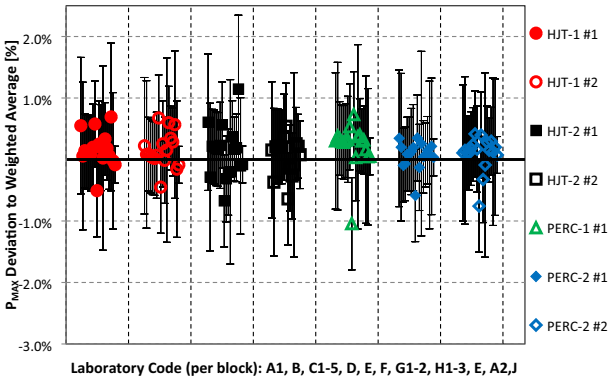

FIGURE 7 Maximum power point deviations to the weighted mean for all modules as measured blindly by each laboratory at predefined I_{SC} condition at 25°C. The estimated values of measurement uncertainty ($k = 2$) are shown as error bars for each laboratory. For DUT HJT-2 #2 cell, the measurements submitted by Laboratories I, A2, and J were not accounted due to the terminal damage of DUT. [Colour figure can be viewed at wileyonlinelibrary.com]

varied between 0.61% and 1.48% ($k = 2$) in P_{MAX}. These values indicate good agreement between laboratories. Worst-case agreement in P_{MAX} was seen in measurement of Laboratory I for DUT HJT-2 #1, where the laboratory deviation to the consensus value was higher by 1.15%. Another noticeable difference is the value measured by Laboratory E for sample PERC-1 #1, which deviated by −1.04% in P_{MAX} to the consensus value. These two deviations are most likely single events, which are difficult to explain, as the deviation in the associated value of V_{OC} was less than 0.2% of the consensus value.

3.5 | Open-circuit voltage comparison under predetermined I_{SC}

Laboratory-weighted deviations in V_{OC} remain within 0.28%–0.38% ($k = 2$) for all modules (Figure 8), while the uncertainty of the consensus values of V_{OC} stayed 0.14% ($k = 2$) for all the modules. Generally, these values are encouraging and indicate a high level of agreement observed among the participant laboratories. Worst-case agreement in V_{OC} from the consensus values were the values recorded in the first measurements of Laboratory E for devices PERC-2 #1 and #2, which deviate by −0.44% and −0.48%, respectively. The errors are consistent with the P_{MAX} measurement of the laboratory, which was also underestimated by −0.59% and −0.76% for devices PERC-2 #1 and #2, respectively (Figure 7). It is noted that systematic deviations are observed in results from some laboratories, such as Laboratories E and D; Laboratory D systematically overestimated V_{OC} for all DUTs by 0.21%–0.37% higher than the consensus values, but the reported values were within the uncertainties stated. Since no significant systematic overestimation or underestimation was recorded, it is assumed that all employed methods and procedures are valid.

1099159x, 0, Downloaded from https://onlinelibrary.wiley.com/doi/10.1002/pip.3630 by Universite Lorraine, Wiley Online Library on [04/11/2022]. See the Terms and Conditions (https://onlinelibrary.wiley.com/terms-and-conditions) on Wiley Online Library for rules of use; OA articles are governed by the applicable Creative Commons License

3.6 | Correlation

The results of correlations among deviations of P_{MAX}, V_{OC}, and *FF* compared to their weighted mean are shown in Table 9. A correlation is observed in P_{MAX} and V_{OC} with a correlation coefficient of 0.613, which is mainly attributed to the linear temperature dependence between P_{MAX} and V_{OC} (Figure 9). As for the correlation of *FF* with P_{MAX} and V_{OC}, *FF* and P_{MAX} are strongly correlated ($r = 0.700$), while a weak, but not negligible, linear relationship is seen between *FF* and V_{OC} ($r = 0.223$). Since *FF* is calculated based on V_{OC} and P_{MAX} when I_{SC} is predefined, the measurement deviations of voltage and power have crucial impact on the *FF*. For brevity, only the linearity relationships between P_{MAX} and *FF* are presented here and shown in Figure 10.

The statistical significance of a correlation is used as a diagnostic method to evaluate its impact on the measurement. The statistical significance was evaluated on the basis of evaluating the posterior probability of the null hypothesis, H_0, which assumes that the studied quantities are uncorrelated. The correlation coefficients, their *t*-values, and the significance of H_0 are shown in Table 9. The calculation of *t*-value is bound to 121 degrees of freedom ($v = N - 2$, 123 sets of measurements bound by two coefficients of linear regression). For all cases in Table 9, H_0 clearly does not reach the critical significance of 5%, that is, $P_r(t|H_0) \leq 0.05$, and is therefore rejected. In fact, in all cases, the significance of H_0 stayed below 1.5%, which indicates that the examined pair of quantities, P_{MAX}-V_{OC}, P_{MAX}-*FF*, and V_{OC}-*FF* are significantly correlated. These results prove in terms of statistics the mutual quantitative dependence of performance parameters in round-robin measurement campaigns. It is, however, conceptually important to highlight that the correlation between performance parameters submitted by one laboratory does not imply any dependence between

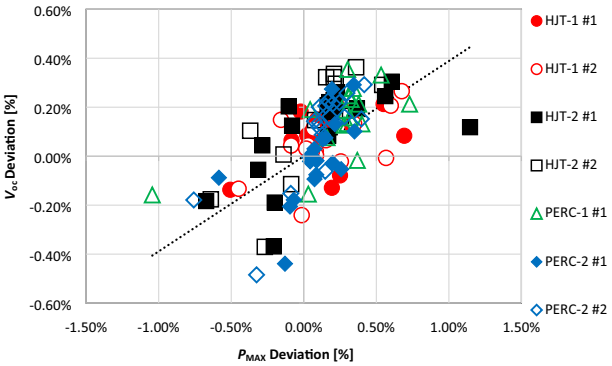

FIGURE 9 Correlation of ΔV_{oc} and ΔP_{MAX} in the round-robin for fixed I_{sc} and 25°C. The high linearity shown here indicates strong dependence of ΔV_{OC} on the measurement deviation of P_{MAX}. The correlation coefficient is 0.613 with statistical significance exceeding 99.9% (Table 9). It is noted that the linear regression coefficient is the same with the correlation coefficient only when all data are normalized. [Colour figure can be viewed at wileyonlinelibrary.com]

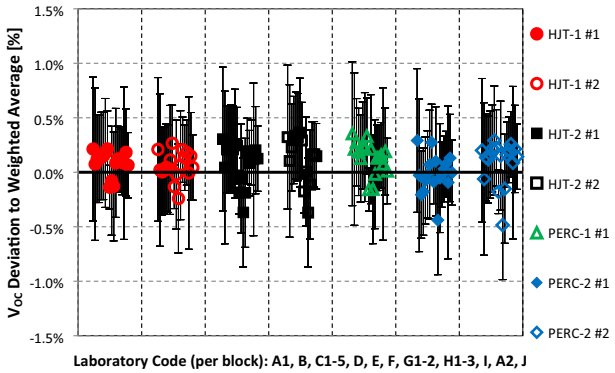

FIGURE 8 Open-circuit voltage deviations to the weighted mean as measured blindly by each laboratory at predefined I_{SC} condition at 25°C. The representations used are the same as in Figure 7. [Colour figure can be viewed at wileyonlinelibrary.com]

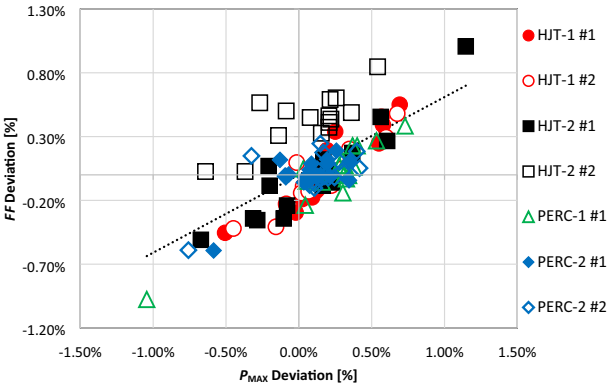

FIGURE 10 Correlation of ΔFF and ΔP_{MAX} in the round-robin for fixed I_{sc} and 25°C. The high linearity shown here indicates strong dependence of ΔFF on the measurement deviation of P_{MAX}. The corresponding correlation coefficient is 0.700 with statistical significance exceeding 99.9% (see Table 9). It is noted that the linear regression coefficient is the same as the correlation coefficient only when all data are normalized. [Colour figure can be viewed at wileyonlinelibrary.com]

TABLE 9 Simplified matrix of correlation coefficients for ΔP_{MAX}, ΔV_{OC}, and ΔFF as calculated from the round-robin results for predefined I_{SC} and 25°C

v = 121	ΔP_{MAX}	ΔV_{OC}	ΔFF
ΔP_{MAX}	1		
t-value (conf.)	-		
ΔV_{oc}	**0.613 ± 0.057**	1	
t-value (conf.)	8.54[a] (<0.01%)	-	
ΔFF	**0.700 ± 0.046**	**0.223 ± 0.0861**	1
t-value (conf.)	10.78[b] (<0.01%)	2.52[b] (1.17%)	-

Notes: Correlation coefficients are shown in bold with their standard error. The *t*-values and their statistical significance (in brackets) are listed. The critical value of the *t*-statistic that corresponds to 95.4% confidence for 121 degrees of freedom is also reported at the bottom.
[a]t-critical = 1.698 (one-tailed, corresponding to 95.4% confidence).
[b]t-critical = 2.016 (two-tailed, corresponding to 95.4% confidence).

1099159x, 0, Downloaded from https://onlinelibrary.wiley.com/doi/10.1002/pip.3630 by Universite Lorraine, Wiley Online Library on [04/11/2022]. See the Terms and Conditions (https://onlinelibrary.wiley.com/terms-and-conditions) on Wiley Online Library for rules of use; OA articles are governed by the applicable Creative Commons License

the test results submitted by different participant laboratories. Therefore, the assumption of independent measurements, which was made to evaluate the results, is still valid.

3.7 | Effect of transient current caused by hysteresis effect on the error of maximum power value

For HE c-Si solar cells, the hysteresis effect, which is caused by the charging and discharging of the capacitance of solar cells in the form of a transient current dQ/dt, will introduce a transient measurement error during the *I*–*V* scanning. As previous research has shown, the transient current can be deduced based on solar cell device physics as[29]:

$$\frac{dQ}{dt} = \left(\frac{q}{kT} \frac{qwn_i^2 \exp\left(\frac{qV_j}{kT}\right)}{\sqrt{N_{A,D}^2 + 4n_i^2 \exp\left(\frac{qV_j}{kT}\right)}} \right) \left(\frac{dV}{dt} + \frac{dJ}{dt} R_S \right) \quad (8)$$

where Q is the per-unit-area charge in the solar cell; $N_{A,D}$ is the substrate doping density; n_i is the intrinsic carrier density; q, w, k, and T are the elementary charge, cell thickness, Boltzmann's constant, and cell temperature, respectively; and V_j, V, J and R_S are the solar cell junction voltage, terminal voltage, current density, and series resistance, respectively; these final variables are related by the lumped series resistance model: $V_j = V + JR_s$. Despite its apparent complexity, Equation (8) expresses a straightforward linear relationship between a few experimental variables (V, J, dV/dt, and dJ/dt) and the transient current (dQ/dt). This is most easily seen by considering the two terms in brackets on the right-hand side of Equation (8) individually.

The first term represents the strength of the linear relationship (i.e., its slope). It largely consists of physical constants and inherent properties of the DUT. Given that temperature has been well controlled in the round-robin, the other remaining experimental variable V_j is defined explicitly if the device R_S is known or is defined implicitly by specifying a single point on the *I*–*V* curve at which to report results. The latter is relevant in this case, where the single specified point is the maximum power point. This first term is therefore treated as constant for a given DUT, which is an assumption that holds true so long as V_j at P_{MAX} is similar for a DUT for all participant laboratories.

The second term represents the junction voltage sweep rate. It largely consists of experimental variables controlled differently by each laboratory, namely, the voltage and current sweep rates employed when measuring the maximum power point of each DUT. The junction voltage sweep rate depends on the device R_S; since we do not have a consensus value of R_S for each DUT, we have used a nominal constant value for each DUT in the analysis that follows. Interlaboratory comparison of R_S was not a main concern for this round-robin, as standardized methods for measuring this device parameter already exist.

The aim of this analysis is to investigate the effect of transient current on the error of P_{MAX} for HE solar cells. From the above discussion of Equation (8), it follows that a plot of the P_{MAX} error versus the junction voltage sweep rate should be linear for each DUT, with a greater magnitude of slope for devices that are more prone to capacitive errors. The P_{MAX} value here refers to the measurand without hysteresis–elimination correction, and the error on P_{MAX} is the deviation relative to the consensus value applied in the above proficiency test.

As shown in Figure 11, the expected linear relationship is observed with linearity coefficients greater than 0.97 for each HJT solar cell (i.e., HJT-1 #1, HJT-1 #2, and HJT-2 #1). Positive values of the junction voltage sweep rate (which generally correspond to "forward" *I*–*V* sweeps from I_{SC} to V_{OC}) result in under-reporting of P_{MAX}, while negative values of the junction voltage sweep rate result in overreporting of P_{MAX}. When the junction voltage sweep rate remains within ± 3 V s^{-1}, the measured P_{MAX} deviation stays within approximately ±1%.

On the other hand, for PERC solar cells (i.e., PERC-1 #1 and PERC-2 #1 and #2), the expected linear relationship is observed only poorly, with linearity coefficients less than 0.10. Given that the PERC cells are much less prone to capacitive errors than the HJT cells—roughly 50 times less, by comparing the slopes in Figure 11—the poor correlation may be because the linear trends in the PERC data are overshadowed by other factors not related to capacitive errors. This may also explain why the fit lines for the PERC cells do not cross the origin as Equation (8) would predict. Despite this, the slopes of the linear fit lines nevertheless have the correct sign, such that positive values of the junction voltage sweep rate result in lower reported values of P_{MAX}, which is the same behavior as the HJT cells. Finally, the P_{MAX} deviations of PERC-2 are generally larger than that of PERC-1 for a given junction voltage sweep rate. This may be attributed to the intrinsic difference between PERC-1 and PERC-2 solar cells and also probably because of the stability issues of PERC-2.

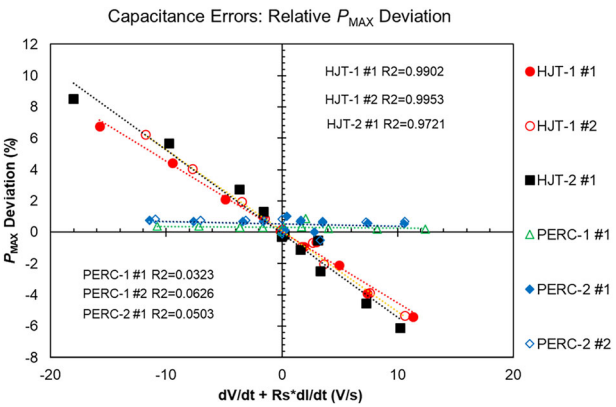

FIGURE 11 Relationship between P_{MAX} deviation and junction voltage sweep rate at maximum power point for all solar cells and selected laboratories. All data appearing on the graph are uncorrected for device hysteresis. [Colour figure can be viewed at wileyonlinelibrary.com]

1099159x, 0, Downloaded from https://onlinelibrary.wiley.com/doi/10.1002/pip.3630 by Universite Lorraine, Wiley Online Library on [04/11/2022]. See the Terms and Conditions (https://onlinelibrary.wiley.com/terms-and-conditions) on Wiley Online Library for rules of use; OA articles are governed by the applicable Creative Commons License

This analysis essentially confirms the relation between the transient current that is the root cause of hysteresis effects and the uncorrected P_{MAX} deviation for various HE c-Si solar cells, consistent with results reported elsewhere.[30] The analysis can be used to determine the range of junction voltage sweep rates for a given DUT type that will give acceptably small errors for the uncorrected P_{MAX} values. The analysis does not consider numerical corrections applied to P_{MAX} values after measurement, although several correction procedures of varying complexity derived from various hysteresis models exist in the literature,[3,10,11] and such corrections are not excluded by the current analysis.

4 | CONCLUSIONS

A round-robin interlaboratory comparison was realized between 10 laboratories based in Asia, Europe, and North America. The participants were five ISO/IEC 17025 accredited laboratories (three for calibration and two for testing) and five industrial laboratories. The scope of this work was to examine the comparability of measurements made by different laboratories utilizing different procedures on the measurement of HE solar cells with particular focus on voltage sweeping methods. The sweeping methods examined in this work are (i) linear sweep rate, (ii) nonlinear sweep rate, (iii) hysteresis measurement and correction, (iv) voltage-stepping correction, and (v) voltage-irradiance modulation and correction. Furthermore, the work aimed to compare different methods and laboratory setups used between ISO/IEC 17025 accredited calibrations and testing as well as industrial laboratories that have processes and procedures in place in accordance with IEC 60904-1.

A proficiency test was employed to examine the consistency of results and their corresponding uncertainties but also isolate possible outliers. For all stable devices, the results of all participant laboratories generally remained well within [−1; 1], thus indicating consistency between the measured values and the reference within the declared UCs for all measurement procedures and laboratories. The reference values were obtained by calculating the weighted average of submitted data by ISO/IEC 17025 accredited laboratories. The deviations of I_{SC} under STC remained within ±1.7% for four accredited laboratories, and this deviation was affected by the stability issues of DUTs and the systematic errors of participant laboratories to some degree. For the measurements under predefined I_{SC}, the maximum measured deviations varied for all stable samples within ±0.59% to ±1.15% for P_{MAX} and within ±0.21% to ±0.48%, for V_{OC}. The weighted deviations per sample type ranged within ±0.61% to ±1.48% ($k = 2$) for P_{MAX} and ±0.35% to ±0.46% ($k = 2$) for V_{OC}, which can be seen as a conservative estimation of interlaboratory agreement of this round-robin. Correlations were observed among the P_{MAX}, V_{OC}, and *FF* differences from their weighted mean. The dependence of temperature deviation was identified as a main factor resulting in a relatively strong ($r = 0.60$) and significant correlation between ΔP_{MAX} and ΔV_{OC}. These numbers are encouraging and indicate good agreement for all participants. Essentially, this work validated all applied methods and their stated measurement uncertainties.

The effect of transient current that is the root cause of hysteresis effects was analyzed for the maximum power value error of each solar cell. The results match theoretical predictions for all HJT solar cells, and in particular, the maximum absolute deviations to the weighted mean for P_{MAX} could be reduced within ±1% for all the DUTs using a junction voltage sweep rate within ±3 V s^{-1}. Meanwhile, for the PERC solar cells with significantly less capacitance effect, the results only somewhat matched theoretical predictions. This indicates the extent to which different HE c-Si solar cell technologies have different propensity for capacitive errors and therefore require more or less careful attention in order to reduce the error in the maximum power measurement.

DATA AVAILABILITY STATEMENT

Research data are not shared.

ORCID

Christos Monokroussos https://orcid.org/0000-0002-6953-0638
Diego Pavanello https://orcid.org/0000-0001-6736-6670
Qi Gao https://orcid.org/0000-0001-6230-9116
Yi Feng Chen https://orcid.org/0000-0001-8601-0979

REFERENCES

1. Ossenbrink HA, Zaaiman W, Bishop J. Do multi-flash solar simulators measure the wrong fill factor? In: *23rd IEEE Photovoltaic Specialists Conference*; 1993:1194-1196. doi:10.1109/PVSC.1993.346953
2. Friesen G, Ossenbrink HA. Capacitance effects in high-efficiency cells. *Sol Energy Mater Sol Cells*. 1997;48(1-4):77-83. doi:10.1016/S0927-0248(97)00072-X
3. Metzdorf J, Meier A, Winter S, Wittchen T. Analysis and correction of errors in current-voltage characteristics of solar cells due to transient measurements. In: *12th European photovoltaic solar energy conference (EUPVSEC)*; 1994:496-499.
4. Hishikawa Y. Precise performance measurement of high-efficiency crystalline silicon solar cells. In: *4th IEEE World Conference on Photovoltaic Energy Conversion*; 2006:1279-1282. doi:10.1109/WCPEC.2006.279647
5. Monokroussos C, Gottschalg R, Tiwari AN, Friesen G, Chianese D, Mau S. The effects of solar cell capacitance on calibration accuracy when using a flash simulator. In: *4th IEEE World Conference on Photovoltaic Energy Conversion*; 2006:2231-2234. doi:10.1109/WCPEC.2006.279953
6. Virtuani A, Müllejans H, Dunlop ED. Comparison of indoor and outdoor performance measurements of recent commercially available solar modules. In: *23rd European Photovoltaic Solar Energy Conference (EUPVSEC)*; 2008:2713-2718.
7. Sinton RA. A solution to the problem of accurate flash-testing of high-efficiency modules. In: *21st European Photovoltaic Solar Energy Conference*; 2006.
8. Monokroussos C, Etienne D, Morita K, Dreier C, Therhaag U, Herrmann W. Accurate power measurements of high capacitance PV modules with short pulse simulators in a single pulse. In: *27th European Photovoltaic Solar Energy Conference (EUPVSEC)*; 2012.
9. Gao Q, Zhang Y, Yu Y, Liu Z. Effects of I–V measurement parameters on the hysteresis effect and optimization in high-capacitance PV module testing. *IEEE J Photovolt*. 2018;8(3):710-718. doi:10.1109/JPHOTOV.2018.2810852
10. Virtuani A, Rigamonti G, Friesen G, Chianese D, Beljean P. Fast and accurate methods for the performance testing of highly-efficient c-Si

1099159x, 0, Downloaded from https://onlinelibrary.wiley.com/doi/10.1002/pip.3630 by Universite Lorraine, Wiley Online Library on [04/11/2022]. See the Terms and Conditions (https://onlinelibrary.wiley.com/terms-and-conditions) on Wiley Online Library for rules of use; OA articles are governed by the applicable Creative Commons License

photovoltaic modules using a 10 ms single-pulse solar simulator and customized voltage profiles. *J Meas Sci Technol*. 2012;23(11):115604. doi:10.1088/0957-0233/23/11/115604

11. Kojima H, Iwamoto K, Shimono A, Abe J, Hishikawa Y. Accurate and rapid measurement of high-capacitance PV cells and modules using a single short pulse light. In: *IEEE 40th Photovoltaic Specialist Conference (PVSC)*; 2014:1896-1898. doi:10.1109/PVSC.2014.6925295
12. Ramspeck K, Schenk S, Komp L, Metz A, Meixner M. Accurate efficiency measurements on very high efficiency silicon solar cells using pulsed light sources. In: *29th European Photovoltaic Solar Energy Conference (EUPVSEC)*; 2014.
13. Monokroussos C, Yoshita M, Yamagoe K, et al. Interlaboratory comparison of voltage sweep methods used for the electrical characterization of encapsulated high-efficiency c-Si solar cells. In: *38th European Photovoltaic Solar Energy Conference (EUPVSEC)*; 2021.
14. IEC 60904-1:2020. Photovoltaic devices - part 1: measurement of photovoltaic current-voltage characteristics.
15. Betts TR, Zdanowicz T, Prorok M, et al. Photovoltaic performance measurements in Europe: PV-catapult round robin tests. In: *4th IEEE World Conference on Photovoltaic Energy Conversion*; 2006:2238-2241. doi:10.1109/WCPEC.2006.279955
16. Herrmann W, Mau S, Fabero F, et al. Advanced intercomparison testing of PV modules in European test laboratories. In: *22nd European Photovoltaic Solar Energy Conference (EUPVSEC)*; 2006:2506-2510.
17. Hishikawa Y, Liu H, Hsieh H-H, et al. Round-robin measurement intercomparison of c-Si PV modules among Asian testing laboratories. *Prog Photovolt Res Appl*. 2013;21(5):1181-1188. doi:10.1002/pip.2255
18. Dirnberger D, Kräling U, Müllejans H, et al. Progress in PV module calibration – results of a world-wide intercomparison between four reference laboratories. *Meas Sci Technol*. 2014;25(10):105005. doi:10.1088/0957-0233/25/10/105005
19. Salis E, Pavanello D, Field M, et al. Improvements in world-wide intercomparison of PV module calibration. *Sol Energy*. 2017;155:1451-1461. doi:10.1016/j.solener.2017.07.081
20. Monokroussos C, Salis E, Etienne D, et al. Electrical characterization intercomparison of high-efficiency c-Si modules within Asian and European laboratories. *Prog Photovolt Res Appl*. 2019;27(7):603-622. doi:10.1002/pip.3134
21. IEC 60904-4: 2019. Photovoltaic devices - part 4: photovoltaic reference devices - procedures for establishing calibration traceability.
22. ISO/IEC 17043:2010, conformity assessment - general requirements for proficiency testing.
23. Cox MG. The evaluation of key comparison data. *Metrologia*. 2002;39(6):589-595. doi:10.1088/0026-1394/39/6/10
24. Cox MG, Eiø C, Mana G, Pennecchi F. The generalized weighted mean of correlated quantities. *Metrologia*. 2006;43(4):S268-S275. doi:10.1088/0026-1394/43/4/S14
25. Müllejans H, Zaaiman W, Dunlop ED. Reduction of uncertainties for photovoltaic reference cells. *Metrologia*. 2015;52(5):646-653. doi:10.1088/0026-1394/52/5/646
26. Dietrich CF. *Uncertainty, calibration and probability*. Ed. 2 ed; 1991:37-42.
27. Van Elst H. Foundations of descriptive and inferential statistics; 2015. doi:10.48550/arXiv.1302.2525
28. Kendall MG, Stuart A. *The Advanced Theory of Statistics*. Vol. 2: Inference and Relationship. Charles Griffin; 1973.
29. Sinton RA, Wilterdink HW, Blum AL. Assessing transient measurement errors for high-efficiency silicon solar cells and modules. *IEEE J Photovolt*. 2017;7(6):1591-1595. doi:10.1109/JPHOTOV.2017.2753200
30. Blum AL, Sinton RA, Wilterdink HW. Determining the accuracy of solar cell and module measurements on high-capacitance devices. In: *IEEE 7th World Conference on Photovoltaic Energy Conversion (WCPEC)*; 2018:3603-3606. doi:10.1109/PVSC.2018.8548016

How to cite this article: Zhang Y, Monokroussos C, Wilterdink H, et al. Interlaboratory comparison of voltage sweep methods used for the electrical characterization of encapsulated high-efficiency c-Si solar cells. *Prog Photovolt Res Appl*. 2022;1-14. doi:10.1002/pip.3630

1099159x, 0, Downloaded from https://onlinelibrary.wiley.com/doi/10.1002/pip.3630 by Universite Lorraine, Wiley Online Library on [04/11/2022]. See the Terms and Conditions (https://onlinelibrary.wiley.com/terms-and-conditions) on Wiley Online Library for rules of use; OA articles are governed by the applicable Creative Commons License